AVAILABLE ON THE HEI WEBSITE

Research Report 195

Impacts of Regulations on Air Quality and Emergency Department Visits in the Atlanta Metropolitan Area, 1999–2013

Russell et al.

APPENDIX E. LINKED RESPONSE OF AEROSOL ACIDITY AND AMMONIA TO SO_2 AND NO_x EMISSIONS REDUCTIONS IN THE U.S.: A FOCUS ON THE SOUTHEAST

This Appendix was reviewed solely for spelling, grammar, and cross-references to the main text. It has not been formatted or fully edited by HEI. This document was reviewed by the HEI Review Committee.

Correspondence may be addressed to Dr. Armistead (Ted) Russell, Department of Civil and Environmental Engineering, Georgia Institute of Technology, 311 Ferst Drive, Atlanta, GA 30322; e-mail: *trussell@ce.gatech.edu*.

Although this document was produced with partial funding by the United States Environmental Protection Agency under Assistance Award CR–83467701 to the Health Effects Institute, it has not been subjected to the Agency's peer and administrative review and therefore may not necessarily reflect the views of the Agency, and no official endorsement by it should be inferred. The contents of this document also have not been reviewed by private party institutions, including those that support the Health Effects Institute; therefore, it may not reflect the views or policies of these parties, and no endorsement by them should be inferred.

APPENDIX E. LINKED RESPONSE OF AEROSOL ACIDITY AND AMMONIA TO SO_2 AND NO_X EMISSIONS REDUCTIONS IN THE UNITED STATES: A FOCUS ON THE SOUTHEAST

Contents

SUMMARY

Large reductions of sulfur dioxide and nitrogen oxide emissions in the United States have led to equally impressive improvements in air quality, including lowered ambient fine particulate matter (PM) and ozone gas levels, though recent analyses in the southeastern United States show aerosol pH is much less responsive. In this study, aerosol acidity is examined on a nationwide scale using ambient concentration data from three monitoring networks — AMoN, CASTNET and SEARCH — along with thermodynamic (ISORROPIA II) and chemical transport (CMAQ) models to predict aerosol acidity. Results show that sulfate and ammonium have similar and significant decreases, with little or no pH change. At SEARCH sites, which are situated mainly in the Southeast, small increases in pH (+0.003 to 0.09 pH units/season) were observed at all sites except for CTR* (–0.0026 pH units/season). From the nationwide CASTNET/AMoN networks, only one out of all five regions, California, exhibited a statistically significant, but still small, pH change with an annual increase of +0.04 pH/yr (est +5.2%). CMAQ calculations led to similar responses, showing generally low pH nationally with little change in aerosol pH or ammonia levels from 2001 to 2011.

*Abbreviations for the SEARCH sites are listed at the end of this appendix.

INTRODUCTION

Atmospheric aerosols, such as fine particulate matter like $PM_{2.5}$ have become a focus of increasing attention due to their significant and adverse effects on global atmospheric processes (e.g., radiative transfer, cloud formation) and atmospheric chemistry, but also because they have significant adverse impacts on human health and morbidity. (Abbatt et al. 2006; Charlson et al. 1992; Martin et al. 2004; Pope and Dockery 2006; Utell and Frampton 2000; Valavanidis et al. 2008; Zhang et al. 2015). A key property of the aerosol is its acidity, which plays a critical role in heterogeneous chemistry (e.g., secondary aerosol formation, metal dissolution, and nitrate/nitric acid partitioning) and has been linked to adverse health effects (Delfino et al. 2005; Fan and Jacob 1992; Ghio et al. 2012; Kleinman et al. 1989; Meskhidze et al. 2003; Thurston et al. 1994; Utell 1985; Xu et al. 2015). The role that aerosol acidity plays in affecting climate forcing may also be substantial as particle pH is known to affect radiative forcing (Fisher et al. 2011; Ritter et al. 2005) and can also indirectly affect cloud formation properties (Abbatt et al. 2006).

Aerosol acidity is largely affected by the presence of sulfate and nitrate (SO_4^{2-}, NO_3^-) particulates, which are formed by the oxidization of sulfur and nitrogen oxides (SO_x and NO_x) in the atmosphere. The acidity contributed by these compounds is neutralized, at least to some degree, by reactions with ammonia gas, and the presence of other cations. The question arises as to how aerosol pH has responded to emissions changes over time in light of large decreases in both SO_x and NO_x emissions, the two main precursors to ambient acids. Further, how have ammonia gas levels also responded, given the role ammonia plays in aerosol neutralization and nitrogen deposition? Additionally, did the observed reductions in SO_4^{2-} aerosol lead to reduced acidity, nationally, and to an increase in aerosol NO_3^- levels?

Effects of SO_x and NO_x and their precursor emissions on aerosol acidity and concentration have been studied previously (Blanchard et al. 2011, 2013; Huang et al. 2011; Pathak et al. 2004; Saylor et al. 2015). In one particular study for instance, the researchers reported seeing a decrease in ammonium concentration levels within $PM_{2.5}$ along with an increase in the proportion of ammonia in the gas phase, which would support the effect of decreased emissions seen with SO_x and NO_x (Saylor et al. 2015). Results like these appear to bode well for the possibility of reversing the impacts of acidic aerosols in the atmosphere, as past studies and research have shown that there are high correlations between pH and SO_4^{2-} concentrations in aerosols (Lipfert and Wyzga 1993). However, some studies have shown things to be otherwise. Recently Weber and colleagues (2016) conducted a thermodynamic analysis for pH in the summer at the Centreville site in Alabama and concluded that particles will remain highly acidic until SO_4^{2-} levels decrease to preindustrial levels.

In this study, trends in ammonia, speciated aerosol concentrations, and aerosol acidity in the United States are examined. While aerosol pH is not readily measured, a number of thermodynamic models such as SCAPE (Kim et al. 1993), AIM (Wexler 1991) or the one used in this study, ISORROPIA II (Fountoukis and Nenes 2007) can be employed using concentrations of key constituents within the

aerosol-gas system to predict pH. Data obtained from the AMoN, CASTNET, and SEARCH networks are used as inputs to ISORROPIA II to obtain aerosol pH. The Ammonia Monitoring Network (AMoN) collects ammonia gas concentration across the United States. The Clean Air Status and Trends network (CASTNET) measures $PM_{2.5}$ concentrations across the United States, and the Southeast Aerosol Research and Characterization (SEARCH) provides both ammonia and $PM_{2.5}$ data, though for a limited number of sites in the southeastern United States. In addition, a chemical transport model simulation, in this case the Community Multiscale Air Quality (CMAQ), was also used to provide information over a geographically wide domain. Thus, by separately using data from AMoN (2011–present), CASTNET (2011–present), SEARCH (2008–present), and the Community Multiscale Air Quality (CMAQ) modeling system (2001 and 2011) to (1) investigate spatial and temporal trends of ammonia and $PM_{2.5}$ in the United States, (2) examine how aerosol acidity responds to reduction of SO_4^{2-}, and (3) conduct a parallel analysis using both observation data and thermodynamic modeling, valuable insight into the impact of reduced sulfur emissions on aerosol acidity will be achieved.

METHODS AND DATA SOURCES

Thermodynamic Modeling: ISORROPIA II

ISORROPIA II is a thermodynamic model that predicts the physical phase and chemical composition of inorganic atmospheric aerosol (Nenes et al. 1998). Taking the aerosol-gas phase system as a closed system, ISORROPIA II predicts aerosol acidity (pH) and phase partitioning concentration distributions of the constituents within the system. In forward mode, known quantities such as temperature, relative humidity (RH) and total (gas + aerosol) concentrations are used. In this case, the precursor gases, namely ammonia, sulfuric acid, and nitric acid, which can exist in either phase or both at the same time, are given as total ammonia ($NH_3 + NH_4^+$), total nitrate ($HNO_3(g) + NO_3^-$), and total sulfate ($H_2SO_4 + SO_4^{2-}$). The rest of the constituents, namely the base cations of magnesium, potassium, sodium, and anions (chloride) are also entered as total inputs in ionic form (i.e., Mg^{2+}, Cl^-). The reverse mode is similar but only requires concentrations of the aerosol constituents. For both modes, ISORROPIA II calculates equilibrium concentrations in the gas and aerosol. The user can specify the aerosol to be either in a thermodynamically stable state, where salts precipitate if saturation is exceeded, or in a metastable state, where salts do not precipitate under supersaturated conditions. Here, the forward and metastable modes are used with the seasonal averages of total species concentrations along with temperature and RH from the SEARCH and CASTNET/AMoN databases.

Data Collection CASTNET/AMoN and SEARCH

Due to the sensitivity of temporal and spatial impacts on pH (Lipfert and Wyzga 1993), in order to examine the effect of changing ammonia and SO_4^{2-} levels on pH, all the data from CASTNET and AMoN

sites were first organized according to five different regions (Southeast [SE], Northeast [NE], Midwest [MW], Rocky Mountains [RM], and California [CA]). Afterward, the data from all three networks (i.e., CASTNET, AMoN and SEARCH) were sorted according to the following respective seasons, winter, spring, summer, and fall to compensate for temporal variation. Seasonal averages were then computed defining the seasons as the following months: winter (December to February), spring (March to May), summer (June to August), and fall (September to November).

CASTNET and AMoN

AMoN and CASTNET provide condensed and gas phase species monitoring data for examining the trends of aerosol species concentrations and for modeling of aerosol acidity in ISORROPIA II.

The CASTNET network contains long-term data of air pollutant concentration and deposition and the ecological effects of changing air pollutant emissions. At more than 90 sites across the United States and Canada, weekly ambient measurements are taken for gaseous species (e.g., sulfur dioxide, HNO_3[g]) and condensed phase species (e.g., SO_4^{2-}, NO_3^-, NH_4^+, Mg^{2+}, Ca^{2+}, K^+, Na^+, Cl^-). CASTNET also records daily average temperature and RH. Launched in 2007 and expanded in 2011, AMoN is the only network providing a long-term record of ammonia gas concentrations across the United States. The network uses passive samplers deployed for two weeks, providing biweekly average ammonia concentration at each site. To provide complete ambient measurement input data for ISORROPIA II, which requires total concentration (gas and condensed phase) in forward mode, only colocated CASTNET and AMoN sites as shown in Figure E.1 were selected for this study (additional details can be found in the supplemental tables at the end of this appendix). The lack of gas phase ammonia data from AMoN prior to 2011 limits the study period to March 2011 to February 2016.

Seasonal averages of species concentration and seasonal average temperature and RH are calculated for each site, using the definitions of seasons described earlier. Seasonal total concentration of each species (e.g., TNO_3 [NO_3^- + HNO_3(g)], TNH_3 [NH_3 + NH_4^-] and SO_4^{2-}) are used in ISORROPIA II to model the seasonal average aerosol pH at each site location. Each monitor and its seasonal average species concentrations and seasonal aerosol pH are assigned to one of the following geographic regions: SE, NE, CA, MW, and RK (Figure E.1).

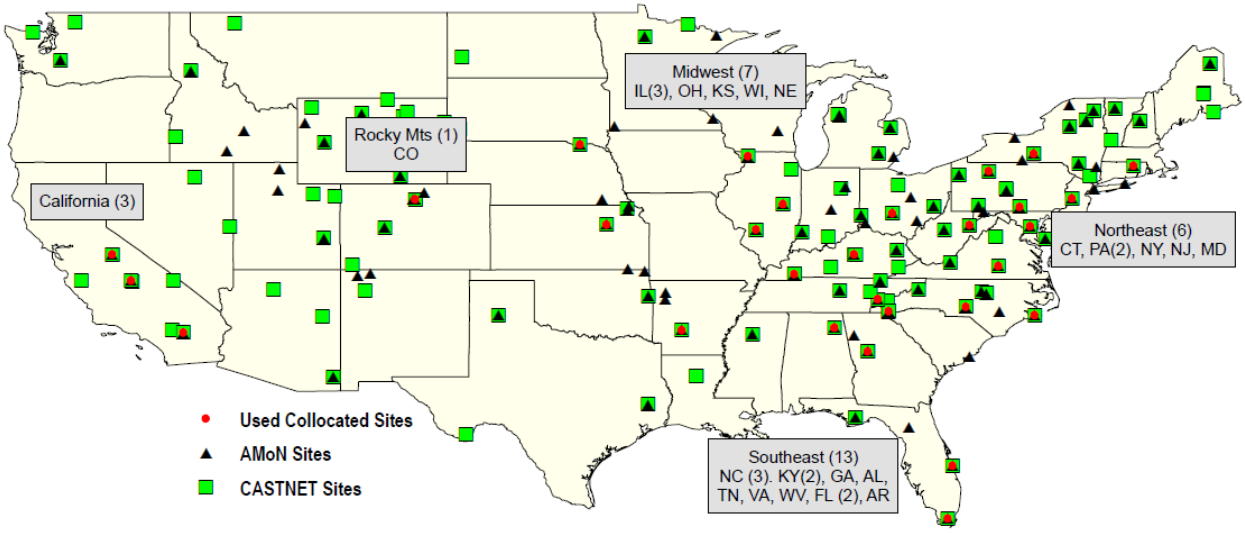

Figure E.1. Spatial map of the CASTNET and AMoN sites, including the co-located CASTNET and AMoN sites used in this study. SEARCH sites were located in the Southeast. (Map source: *Map created using ArcGIS software by ESRI, in conjunction with U.S. EPA data*) (U.S. EPA 2016). Specific site locations are provided in E.S1 and E.S2.

SEARCH

SEARCH is a comprehensive ambient air quality monitoring network designed to gather long-term data in order to characterize, not only the sources of chemical species within particulate matter, but also the spatial and temporal distribution of $PM_{2.5}$ in the southeastern United States. An expansion of SCION, the SEARCH network consists of eight highly instrumented stations located in one pair of urban and rural locations in each of four southeastern states AL, GA, FL, and MS.

Data in SEARCH consists of meteorological, trace gas, and particulate compositional data. Continuous hourly and 24-hour measurements of $PM_{2.5}$, are collected using both on-line and filter-based approaches (e.g., using particle composition monitors [Edgerton 2005]) and are analyzed for particulate species such as SO_4^{2-}, NO_3^-, ammonium (NH_4^+), base cations (Mg^{2+}, Ca^{2+}, K^+, Na^+), and chloride ion (Cl^-) (Edgerton 2005).

The 24-hour data for SO_4^{2-}, NO_3^-, ammonium, chloride, and base cations was used because continuous hourly data were not available. In the case of ammonia, where continuous hourly and 24-hour (sampling frequency- 3-day), trace gas data were available, hourly data (later averaged into a daily value) was used, as more data existed for the hourly than for the daily average. As for ammonia, continuous hourly data were also available for HNO_3 as a trace gas; however, unlike ammonia, nitric acid was also collected as 24-hour measurements together with $PM_{2.5}$ as volatile NO_3^- on nylon backed filters, and thus, the 24-hour volatile NO_3^- was used for nitric acid instead. Details of the available data along with the

sampling frequency are in the supplemental tables at the end of this appendix, and at the SEARCH website.

The continuous hourly data for temperature and RH were collected and later averaged into a daily value. Once the daily averages used for ammonia, temperature, and RH were calculated, the dates for each daily average were matched against the 24-hour $PM_{2.5}$ data. After all the daily data were matched up, the dates for which a complete set of data was available for all the variables were selected, and then seasonal averages were calculated using the seasonal months described earlier.

Prior to 2008, SEARCH did not include base cations, so only data dated from 2008 to 2015 were used; however, not all sites had continuous sets of data available, thereby creating some data gaps. In addition, data collection was discontinued at PNS (2009) and OAK (2011), so the amount of seasonal data points for both sites is substantially smaller than it is for the longer running sites such as the one at JST (additional details are in the supplemental tables at the end of this appendix). However, we still present the data from those sites for completeness.

Chemical Transport Modeling

The CMAQ Model describes the formation and fate of air pollutants over regional areas and uses ISORROPIA II to calculate pH and inorganic species partitioning. Simulations of concentration fields were conducted using the CMAQ (Byun and Schere 2006) version 5.0.2 over the eastern continental United States for 2001 and 2011, using a grid with a 12 km horizontal resolution and 13 vertical layers (Figure E.2). Emissions were developed using the Sparse Matrix Operator Kernel Emissions (SMOKE) platform, with the NEI for 2002 and 2011, and SMOKE 3.5.1 (CMAS Center 2013; U.S. EPA 2014). The Weather Research Forecast version 3.6.1 (Skamarock et al. 2008) was employed to generate meteorological fields.

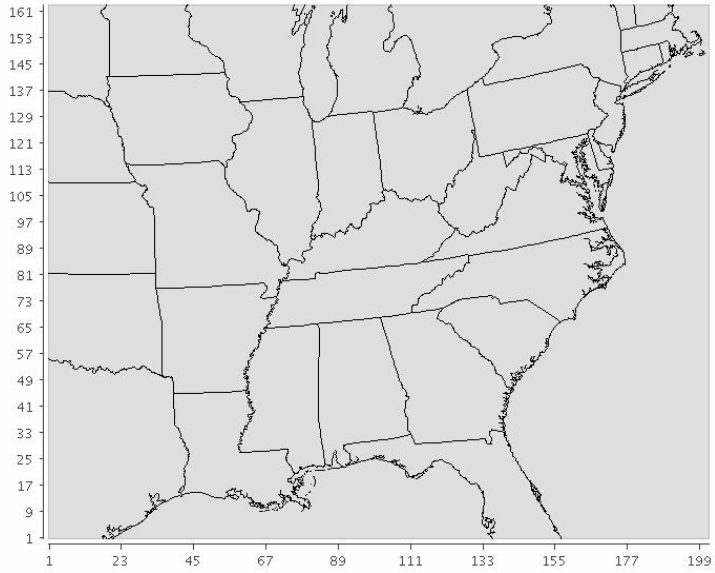

Figure E.2. CMAQ simulation domain with spatial resolution of 12 km.

CMAQ was used to generate seasonal plots of pH and ammonia concentrations in the southeastern, northern and upper midwestern regions for 2001 and 2011 to compare with the results from SEARCH and CASTNET. Lastly, a comparison study of the neutralization ratio with pH in 2011 was conducted as well.

Data Analysis

Time-trend graphs were constructed using seasonal mean values for ambient particulate SO_4^{2-}, particulate NO_3^-, gaseous ammonia, total ammonia, and particulate ammonium (Figures E.4 and E.5). Also plotted were the neutralization ratio R, calculated from observed seasonal molar averages, $R = [NH_4^+]/(2[SO_4^{2-}] + [NO_3^-])$, and model output of pH from ISORROPIA II. All data were plotted as seasonal time series trend, reflecting temporal effects for all variables.

Statistical linear regression analysis and calculations of standard error (*Excel Linest function*) of the slope and intercept were performed to generate 95% confidence intervals (Tables E.1–E.6). The basis for statistical significance for each trend graph was if the slope from the linear regression analysis was outside the margin of error by an order of two standard deviations. The yearly percent changes for each plotted variable were estimated from the slope and intercept obtained from the linear regression equation of each trend plot. Results from the statistical analysis for CASTNET, AMoN and SEARCH are presented in Tables E.1 through E.6.

RESULTS AND DISCUSSION

Despite the majority of all sites and regions in this study exhibiting large reductions in particulate SO_4^{2-}, few large increases in pH were predicted by CMAQ (Figure E.3) or found with ISORROPIA II (Figures E.4a and E.5a). While all SEARCH sites (except CTR) and all areas in the CASTNET/AMoN

network (except Rocky Mountains, which has only one site) from the Southeast, Northeast, Midwest, and California exhibited positive trends for pH, it was only in the Westcoast region (California) from CASTNET (Table E.1) and at the SEARCH site in Oak Grove, Mississippi (Table E.2) where the changes in pH were found to be statistically significant.

Table E.1. Statistical results from the CASNTET/AMoN mean seasonal pH plots for all five regions[a]

pH	Estimated Yearly percent pH change	Years to see 1 pH unit increase
Northeast pH = 0.022 (± 0.018)*t + 2.3 (± 0.21)	+3.9%	9.5
Southeast pH = 0.019(± 0.010)*t + 2.5 (± 0.12)	+3.0%	11.4
Midwest pH = 0.019 (± 0.016)*t + 3.7(± 0.19)	+2.1%	11.6
Rocky Mountains pH = –0.00023 (± 0.019)*t + 2.7 (± 0.22)	+0.034%	NA
California pH =0.038(± 0.015)*t + 2.9 (± 0.18)	**+5.2%**	**5.9**

[a] The equations reflect the seasonal linear trend line constructed for each regional pH plot. The values in parenthesis are the calculated standard error for both slope and intercept. Number of years for 1 pH unit change are calculated using the estimated yearly percentage change and starting intercept value. Results in red were found to be statistically significant. The "t" in all equations refers to time as seasonal counts.

Table E.2. Statistical results from the linear regression analysis for seasonal mean pH at all SEARCH sites[a]

Site[b]	pH	Estimated Yearly percent pH Change	Years to see 1 pH unit change
CTR	pH = –0.0026 (± 0.0071)*t + 1.5 (± 0.10)	–0.70%	N/A
BHM	pH = 0.0022 (± 0.010)*t + 1.9 (± 0.15)	0.44%	94
OLF	pH = 0.0027 (± 0.0038)*t + 1.6 (± 0.064)	0.69%	71
PNS	pH = –0.0091 (± 0.037)*t + 1.8 (± 0.21)	2.0%	22
YRK	pH =0.0042 (± 0.0081)*t + 2.0 (± 0.13)	0.86%	48
JST	pH =0.010 (± 0.0086)*t + 1.8 (± 0.14)	2.3%	20
OAK	**pH =0.091 (± 0.040)*t + 0.76 (± 0.30)**	**48%**	**2.1**
GFP	pH =0.016 (± 0.030)*t + 1.7 (± 0.24)	3.9%	12

[a] The equations reflect the seasonal linear trend line constructed for each regional pH plot. The values in parenthesis are the calculated standard error for both slope and intercept. Number of years for 1 pH unit change are calculated using the estimated yearly percentage change and starting intercept value. Results in red were found to be statistically significant. The "t" in all equations refers to time as seasonal counts.

Analysis of the SO_4^{2-} concentration data from the CASTNET/AMoN networks show that all regions from the Rocky Mountains to the Southeast had substantial yearly reductions in SO_4^{2-} (Table E.3), ranging from estimated values of –6.3% to –9.2%, although the SO_4^{2-} reduction in California was not statistically significant, despite being the only site to have a significant increase in pH.

Table E.3. Tabulated statistical results from the linear regression analysis for mean seasonal sulfate and nitrate concentrations in all five regions in the CASTNET/AMoN network[a]

Sulfate and Nitrate	Estimated Yearly percent change
Sulfate (μg/m³)	
Northeast SO_4^{2-} = –0.053 (± 0.016)*t + 2.4 (± 0.19)	**–8.7%**
Southeast SO_4^{2-} = –0.060(± 0.015)*t + 2.6(± 0.17)	**–9.2%**
Midwest SO_4^{2-} = –0.042(± 0.013)*t + 2.2 (± 0.16)	**–7.5%**
Rocky Mountains SO_4^{2-} = –0.012 (± 0.0057)*t + 0.58 (± 0.069)	**–8.4%**
California SO_4^{2-} = –0.017 (± 0.014)*t + 1.1 (± 0.17)	–6.3%
Nitrate (μg/m³)	
Northeast NO_3^- = 0.011(± 0.022)*t + 0.76 (± 0.26)	+5.6%
Southeast NO_3^- = –0.0015 (± 0.0092)*t + 0.69(± 0.11)	–0.89%
Midwest NO_3^- = 0.0040 (± 0.038)*t + 1.6(± 0.45)	+1.0%
Rocky Mountains NO_3^- = –0.0020 (± 0.0024)*t + 0.20 (± 0.028)	–4.0%
California NO_3^- = –0.0047 (± 0.0099)*t + 0.87 (± 0.12)	–2.2%

[a]The equations reflect the seasonal linear trend lines constructed for each regional plot. The values in parenthesis reflect the standard error for both slope and intercept. Yearly percent changes are estimated from the slope and intercept. Results in red were found to be statistically significant. The "t" in all equations refers to time as seasonal counts.

Comparable SO_4^{2-} results were also observed at SEARCH sites (Table E.4), with all sites (except PNS) showing negative downward trends for SO_4^{2-}, and over 60% of the sites, namely CTR, JST, OLF, YRK and BHM yielding statistically significant reductions ranging in yearly estimated percent reductions from –7.2% to –12%.

Table E.4. Tabulated results for the slope and intercept from the linear regression equation for pH, Neutralization ratio (R), Sulfate (SO_4^{2-}), Nitrate (NO_3^-), Total ammonia (NH_x), Ammonia (gNH_3), Particulate ammonium (NH_4^+), and molar fraction of Ammonia over Total ammonia (gNH_3/NH_x) at all SEARCH sites as listed[a]

Variable	Metric	Units	CTR/AL	GFP/MS	JST/GA	OAK/MS	OLF/FL	YRK/GA	BHM/AL	PNS/FL
pH	Slope(m)/Intercept(b)	pH/Season	–0.0026	0.017	0.0099	**0.091**	0.0027	0.0042	0.0022	0.0091
	Trend Starting Value (b)	pH	1.5	1.7	1.8	**0.76**	1.6	2.0	1.9	1.8
	Percent change (100*4m/b)	%/year	–0.70%	3.9%	2.3%	**48%**	0.69%	0.86%	0.44%	2.0%
R	Rate of change (m)	R/Season	–0.00088	0.012	0.00006	0.011	**0.0041**	–0.002	0.0034	**0.048**
	Trend Starting Value (b)	1/µmol	0.86	0.74	0.93	0.74	**0.78**	0.98	0.86	**0.56**
	Percent change (100*4m/b)	%/year	0.41%	6.5%	0.026%	5.7%	**2.1%**	–0.89%	1.6%	**34.8%**
SO_4^{2-} (µg/m³)	Rate of change (m)	µg/m³/Season	**–0.062**	–0.090	**–0.087**	–0.077	**–0.055**	**–0.13**	**–0.073**	0.089
	Trend Starting Value (b)	µg/m³	**3.0**	3.1	**3.7**	2.9	**3.0**	**4.5**	**3.6**	1.6
	Percent change (100*4m/b)	%/year	**–8.4%**	–12%	**–9.3%**	–11%	**–7.2%**	**–11%**	**–8.1%**	22%
NO_3^- (µg/m³)	Rate of change (m)	µg/m³/Season	0.00049	4.4E-5	0.0026	0.011	0.00065	0.0010	0.0048	0.0069
	Trend Starting Value (b)	µg/m³	0.10	0.14	0.21	0.047	0.11	0.20	0.13	0.15
	Percent change (100*4m/b)	%/year	1.9%	0.13%	4.8%	92%	2.4%	2.0%	15%	18%
NH_4^+ (µg/m³)	Rate of change (m)	µg/m³/Season	**–0.020**	–0.013	**–0.027**	–0.0097	**–0.012**	**–0.044**	**–0.019**	0.057
	Trend Starting Value (b)	µg/m³	**0.96**	0.85	**1.3**	0.81	**0.89**	**1.6**	**1.2**	0.40
	Percent change (100*4m/b)	%/year	**–8.2%**	–6.0%	**–8.3%**	–4.8%	**–5.3%**	**–11%**	**–6.4%**	56%
NH_3 (µg/m³)	Rate of change (m)	µg/m³/Season	0.0014	0.0031	0.0045	0.015	0.0021	–0.012	**–0.033**	–0.025
	Trend Starting Value (b)	µg/m³	0.19	0.55	1.1	0.12	0.28	1.5	**1.9**	0.65
	Percent change (100*4m/b)	%/year	2.9%	2.3%	1.7%	49%	3.0%	–3.1%	**–7.0%**	–15%
NH_X (µg/m³)	Rate of change (m)	µg/m³/Season	**–0.018**	–0.0095	**–0.023**	0.0050	**–0.0097**	**–0.056**	**–0.052**	0.034
	Trend Starting Value (b)	µg/m³	**1.1**	1.4	**2.4**	0.93	**1.2**	**3.2**	**3.1**	1.1
	Percent change (100*4m/b)	%/year	**–6.4%**	–2.7%	**–3.8%**	2.1%	**–3.3%**	**–7.1%**	**–6.8%**	12%
NH_3/NH_X	Rate of change (m)	1/Season	**0.0055**	0.0055	**0.0081**	**0.014**	**0.0051**	**0.0061**	–0.00074	–0.041
	Trend Starting Value (b)	NA	**0.17**	0.40	**0.45**	**0.14**	**0.25**	**0.52**	0.62	0.67
	Percent change (100*4m/b)	%/year	**13%**	5.4%	**7.1%**	**40%**	**8.2%**	**4.7%**	–0.48%	–25%

[a] Yearly percentage changes are estimated from the slope and intercept. Results in red were found to be statistically significant.

The range of SO_4^{2-} concentration across the CASTNET network varied regionally as expected, with the lowest SO_4^{2-} concentrations (based on trend intercept), seen in the Rocky Mountains (0.58 µg/m³) while the SE had an average concentration of 2.6 µg/m³, close to the average concentration of 3.4 µg/m³ from the SEARCH sites. As indicated earlier (see Methods and Data Sources), this result could be attributed to the fact that PNS data did not extend past the year 2009 and therefore, the results from that site should be treated cautiously. Based on the intercept from the linear regression equation, the SO_4^{2-} concentration at all SEARCH sites ranged from lows of 1.6 µg/m³ at PNS and 2.9 µg/m³ at OAK to a high 4.5 µg/m³ at YRK. So in essence, all SO_4^{2-} concentrations, with the exception of PNS, were similar in magnitude.

As stated earlier, despite the drastic SO_4^{2-} reductions, not only did pH not change much, but the values based on the intercept obtained from the linear regression equations for both the SEARCH and CASTNET networks were quite low. For instance, pH values at SEARCH sites ranged from 0.76 in OAK (MS) to a high of 2.0 at YRK (GA), while CASTNET sites yielded pH values with a low of 2.3 in the

Northeast, to a high of 3.7 in the Midwest. Similar pH values were seen with the CMAQ results (Figure E.3), especially in the southeastern and upper midwestern portions of the United States when compared with corresponding areas in SEARCH and CASTNET. The pH in the upper midwestern region appeared to fall between 3.5 and 4.5 through most of the year (except spring) for both years, which matched the Midwest pH of 3.7 from CASTNET/AMoN. The values for the southeast region from the CMAQ results hovered around 1.5–2.0 for the southeastern states, which compared well with the SEARCH site average of 1.6. Furthermore, in addition to the similarities in pH values, an analysis of the pH in the years 2001 and 2011 with CMAQ did not show a drastic change in pH either.

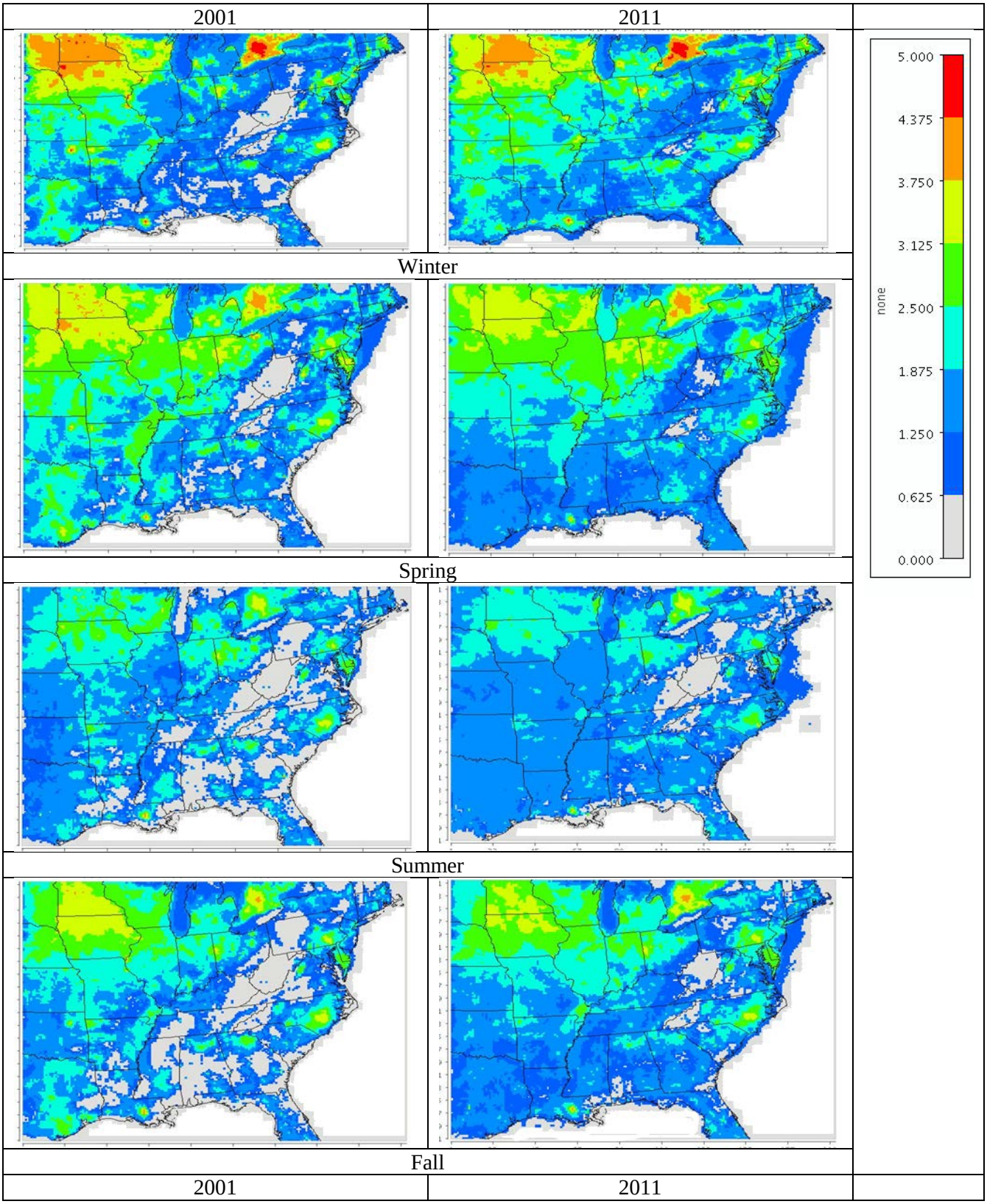

Figure E.3. pH fields based on ion concentration simulated by CMAQ at 2001 and 2011. Simulations were broken into the respective seasons: Winter, Spring, Summer, Fall, to take temporal effects into account.

The observed reduction of SO_4^{2-} was largely accompanied by a similarly noticeable reduction in ammonium. These results (Tables E.4 and E.5), especially those from SEARCH, are consistent with the

observations found in the Southeastern study conducted by Saylor and colleagues (2015) where similar results were reported. In the case of SEARCH, the same sites that had significant decreases in SO_4^{2-} were the only ones to have a significant decrease in ammonium, and the rates of ammonium reduction ranged from –0.012 µg/m^3 NH_4^+/season (est: –5.3%/yr) at OLF to the highest decrease rate at YRK being –0.044 µg/m^3 NH_4^+/season (est: –11%/yr).

The SO_4^{2-} and ammonium results with CASTNET/AMoN did not line up as they did with SEARCH. The highest decrease of ammonium (Table E.5) was in the Northeast with a value of –0.017 µg/m^3 NH_4^+/season (est: –7.3%/yr) to the lowest decrease in California being –0.0076 µg/m^3 NH_4^+/season (est: –6.2%/yr). RK, MW, NE, and SE had significant reductions in SO_4^{2-}, but it was only in the RK, NE, SE, and CA (i.e., not MW) where reductions in ammonium were statistically significant. Part of the difference in the results, with regard to the MW region not having a significant reduction in ammonium as expected, could be because the pH in that region was generally higher and consistently above 3.0, conditions that favor NO_3^- formation. Thus, it is feasible that this is why there was not a significant decrease in ammonium due to the higher NO_3^- concentration. Indeed, as Figure E.4d shows, the concentration of NO_3^- was generally higher, with a trend starting value (Table E.3) of 1.6 µg/m^3 in the MW, well above second highest value 0.87 µg/m^3 for NO_3^-, which was in California. Linear regression analysis was conducted on all NO_3^- trend plots (CASTNET & SEARCH) to see if there was any substantial increase or change in NO_3^- that could explain the changes in the ammonium and ammonia levels. The results for both networks showed no statistically significant change in NO_3^- at any site, indicating that ammonium levels were impacted more by SO_4^{2-} than by NO_3^-, even in the MW. In regards to California, while no significant decrease in SO_4^{2-} or NO_3^- was observed, the significant increase in pH, coupled with the significant decrease in ammonium, could indicate the reduction of other components besides SO_4^{2-} or NO_3^- that might explain the significant decreases there.

Table E.5. Tabulated statistical results from the linear regression analysis for mean seasonal Total ammonia (NH_x), Ammonia (gNH_3), Particulate ammonium (NH_4^+), and molar fraction of Ammonia over Total ammonia (gNH_3/NH_x) in all five regions in the CASTNET/AMoN network[a]

Total Ammonia (NH_x), Ammonia (NH_3), Ammonium(NH_4^+) and Ammonia/Ammonium Molar fraction (NH_3/NH_x)	Estimated Yearly percent change
NH_x ($\mu g/m^3$)	
Northeast NH_x = –0.019 (± 0.0091)*t + 1.7 (± 0.11)	**–4.5%**
Southeast NH_x = 0.0078 (± 0.020)*t + 1.8 (± 0.24)	+1.8%
Midwest NH_x = –0.029 (± 0.023)*t + 3.3 (± 0.28)	–3.6%
Rocky Mountains NH_x = –0.0078 (± 0.018)*t + 0.74 (± 0.14)	–4.2%
California NH_x = 0.019 (± 0.050)*t + 2.4 (± 0.60)	+3.1%
gNH_3 ($\mu g/m^3$)	
Northeast gNH_3 = –0.0021 (± 0.0094)*t + 0.79 (± 0.11)	–1.1%
Southeast gNH_3 = 0.025 (± 0.020)*t + 0.94 (± 0.24)	+11%
Midwest gNH_3 = –0.017 (± 0.026)*t + 2.2 (± 0.31)	–3.1%
Rocky Mountains gNH_3 = –0.0036 (± 0.010)*t + 0.51 (± 0.12)	–2.8%
California gNH_3 = 0.026(± 0.048)*t + 2.0 (± 0.57)	+5.4%
pNH4+ ($\mu g/m^3$)	
Northeast pNH_4^+ = –0.017 (± 0.0068)*t + 0.95 (± 0.082)	**–7.3%**
Southeast pNH_4^+ = –0.017 (± 0.0040)*t + 0.81 (± 0.048)	**–8.4%**
Midwest pNH_4^+ = –0.012(± 0.011)*t + 1.0 (± 0.13)	–4.7%
Rocky Mountains pNH_4^+ = –0.0042 (± 0.0020)*t + 0.23 (± 0.024)	**–7.2%**
California pNH_4^+ = –0.0076 (± 0.0034)*t + 0.49 (± 0.041)	**–6.2%**
NH_3/NH_x ($\mu g/m^3$)	
Northeast NH_3/NH_x = 0.0038 (± 0.0046)*t + 0.47 (± 0.055)	+3.3%
Southeast NH_3/NH_x = 0.0098 (± 0.0036)*t + 0.54 (± 0.043)	**+7.2%**
Midwest NH_3/NH_x = 0.00085(± 0.0047)*t + 0.68 (± 0.056)	+0.50%
Rocky Mountains NH_3/NH_x = 0.0038 (± 0.0029)*t + 0.67 (± 0.035)	+2.3%
California NH_3/NH_x = 0.0040 (± 0.0025)*t + 0.79 (± 0.030)	+2.0%

[a] The equations reflect the seasonal linear trend lines constructed for each regional plot. The values in parenthesis reflect the standard error for both slope and intercept. Yearly percent changes are estimated from the slope and intercept. Results in red were found to be statistically significant. The "t" in all equations refers to time as seasonal counts.

So far, the results from the SO_4^{2-} and ammonium trends corroborate the presumption that more ammonium will partition into ammonia as aerosol SO_4^{2-} levels decrease, but just as with pH, statistically insignificant trends were also observed in regard to the ammonia partitioning changes and total ammonia. For CASTNET/AMoN (Table E.5, Figure E.4e), the results for gaseous ammonia in all regions from 2011 to 2015 remained fairly stable overall with no appreciable change. The total ammonium trend for RK, MW, and NE showed seasonal decreases in total ammonia concentration by –0.0078 $\mu g/m^3$/season, –0.029 $\mu g/m^3$/season and –0.019 $\mu g/m^3$/season respectively, which amounted to estimated percent yearly decreases of about –4.1% for all 3 regions. Conversely, the SE and California regions exhibited seasonal increases in the total ammonia by +0.0078 $\mu g/m^3$/season (est: 1.8%/yr) and +0.019 $\mu g/m^3$/season (est: 3.1%/yr) as opposed to decreases. However, as the slope from the linear trends in all regions (except the

NE) failed to fall two standard deviations outside the margin of error, the changes, while somewhat substantial, were in essence, inconsequential. Data with SEARCH as shown in Table E.4 in regard to the same concentrations were a bit different. A total of five sites showed statistically significant seasonal decreases in total ammonia ranging from –0.0097 μg/m^3/season (est: –3.3%/yr) to –0.056 μg/m^3/season (est: –7.1%/yr) at CTR, JST, OLF, YRK, and BHM, but no statistical change in gaseous ammonia concentration at all sites except at BHM (–0.0033 μg/m^3/season, est: –7.0%/yr). This negative downward trend result for total ammonia was also observed in the same study by Saylor and colleagues (2015), mentioned earlier.

Comparable results for ammonia are noted with CMAQ as well. As shown in Figure E.6, the seasonal gaseous ammonia predictions by CMAQ show a relatively steady concentration of ammonia over the 10-year period. The most noticeable CMAQ ammonia concentration result was a decrease in the amount of red (areas of high concentration) for winter concentrations in the northern region. Other than that, there did not appear to be major changes with ammonia overall.

Despite the trend in gaseous and total ammonia being varied across all sites and regions, there was a noticeable and consistent increase in the molar concentration ratio of gaseous ammonia over total ammonia at all SEARCH (except PNS and BHM), and CASTNET/AMoN sites (Tables E.4 and E.5), another trend also noted by Saylor and colleagues (2015). This seasonal trend of increased gaseous ammonia fraction was again, especially significant at over 60% of SEARCH sites, CTR, JST, OAK, OLF, and YRK and only in the southeast region from the CASTNET/AMoN network. Thus, the combination of the increased proportion of ammonia in the gas phase, coupled with the insignificant change in gaseous ammonia concentration and general decrease in total ammonia would seem to indicate that more ammonium is indeed partitioning into the gaseous phase with reduced SO_4^{2-} levels.

Figure E.4: Mean seasonal time series trends for CASTNET and AMoN co-located sites labeled as follows, **4a**: pH **4b**: Neutralization Ratio calculated from observed concentration. **4c**: Sulfate concentration. **4d**: Nitrate concentration. **4e**: Ammonia concentration. **4f**: Ammonium concentration. **4g**: Ammonia molar fraction over total ammonia. **4h**: Total ammonia concentration.

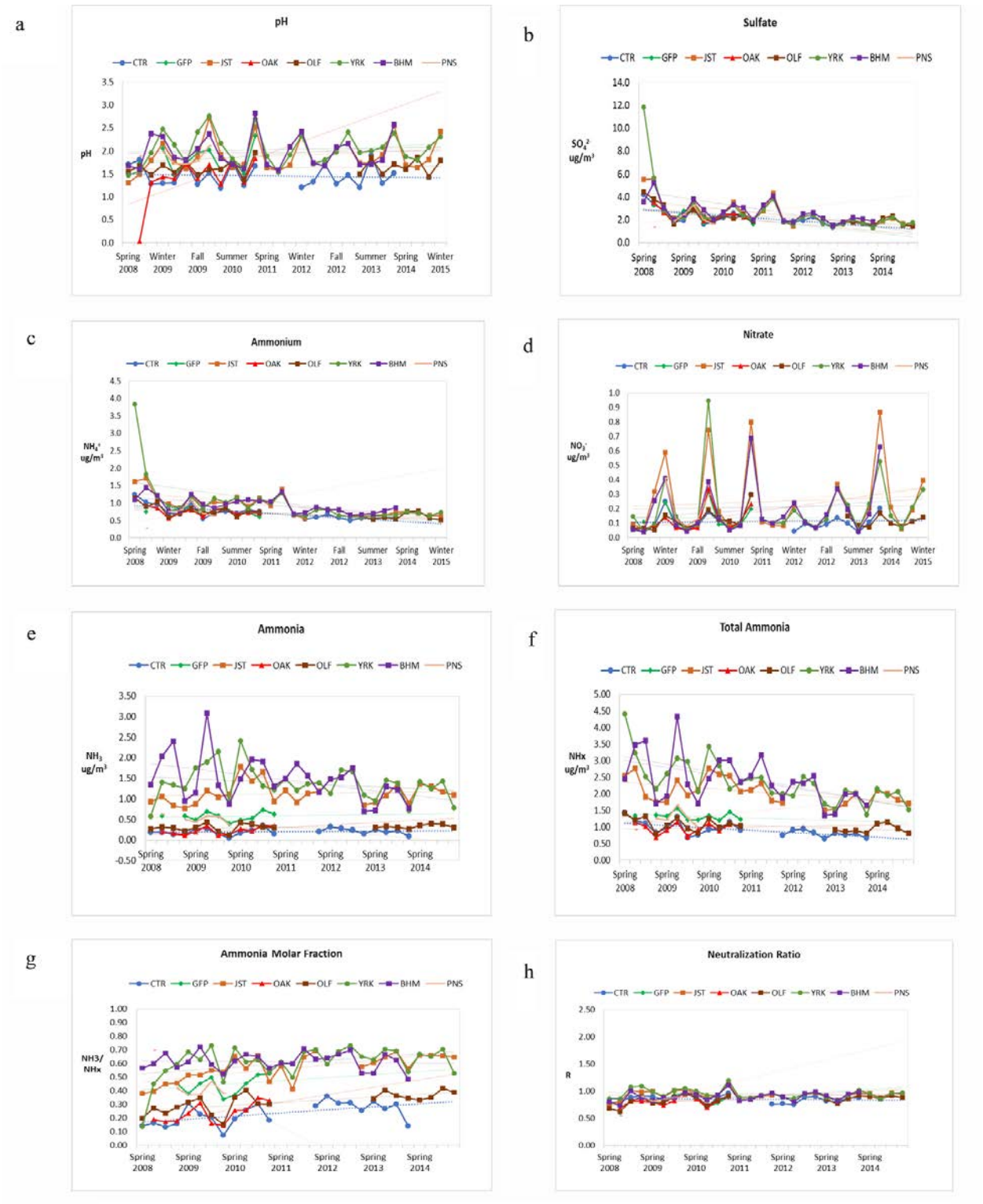

Figure E.5. Mean seasonal time series trends SEARCH sites labeled as follows. 5a: pH **5b:** Sulfate concentration **5c:** Ammonium concentration. **5d:** Nitrate concentration. **5e:** Ammonia concentration. **5f:** Total ammonia. **5g:** Ammonia molar fraction over total ammonia. **5h:** Neutralization Ratio calculated from observed concentrations.

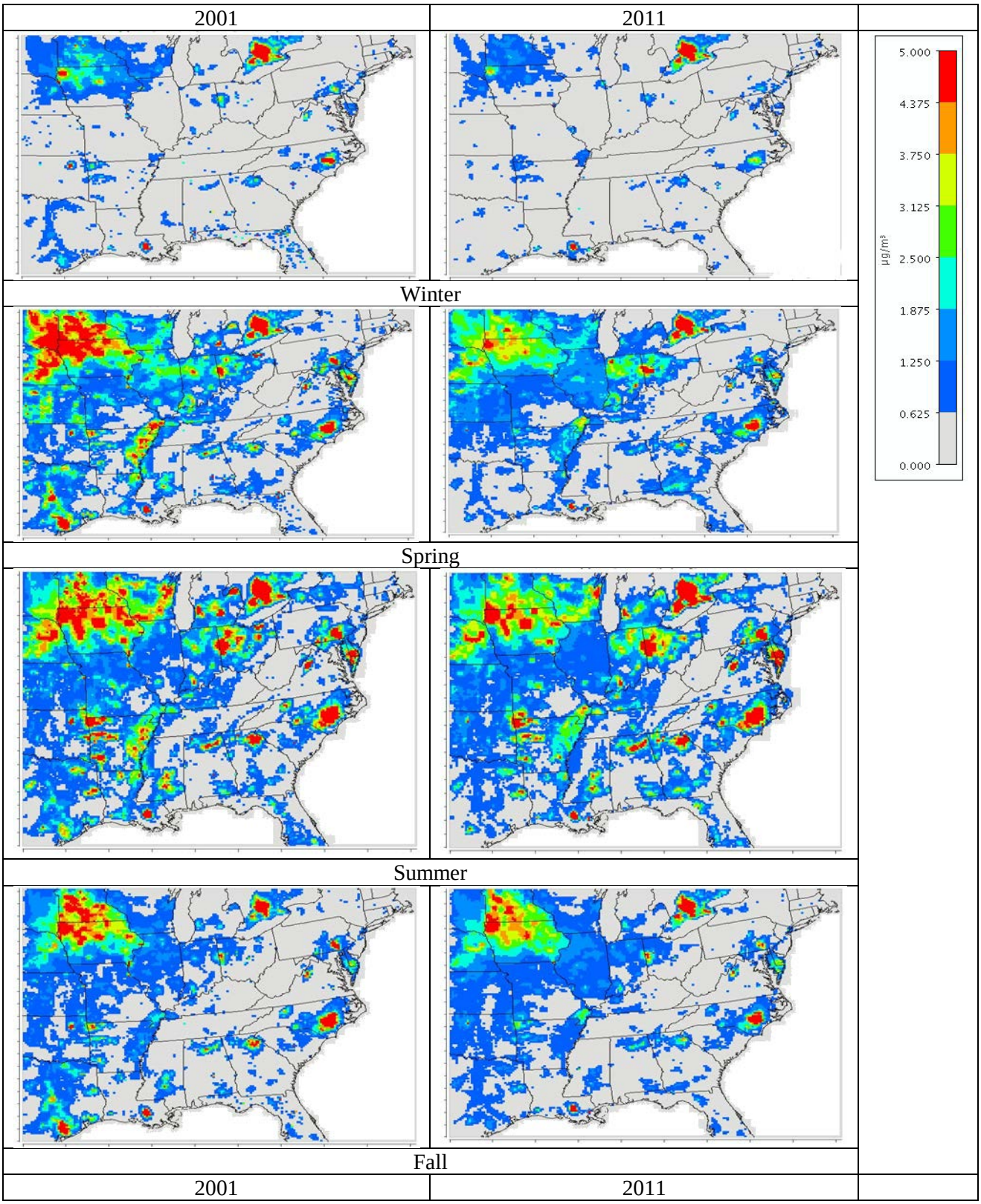

Figure E.6. Ammonia concentration simulated by CMAQ at 2001 and 2011. Simulations were run seasonally (Winter, Spring, Summer, Fall) to take temporal effects into account.

The results so far appear to corroborate the impact of reduced sulfur oxide emissions on particulate matter but its minimal impact on aerosol acidity. Also, not impacted by the reduced emission and SO_4^{2-} levels was the neutralization ratio (Tables E.4 and E.6). The results from the CASTNET/AMoN network did not yield any statistically significant change in this metric, nor was there any change with the majority of the SEARCH sites with the exception of OLF and PNS, both sites in Florida.

Table E.6. Tabulated statistical results of the linear regression analysis of the neutralization ratio calculated for all five regions from the CASTNET/AMoN network with seasonal mean measured concentrations[a]

Neutralization Ratio(R)
Northeast R = –0.0041(± 0.0030)*t + 0.84 (± 0.027)
Southeast R = 3.9E-5 (± 0.0023)*t + 0.68 (± 0.021)
Midwest R = –0.0028 (± 0.0034)*t + 0.82 (± 0.036)
Rocky Mountains R = –0.00030(± 0.0058)*t + 0.86 (± 0.053)
California R = –0.0031(± 0.0061)*t + 0.75 (± 0.056)

[a] The values in parenthesis reflect the standard error for both slope and intercept. The "t" in all equations refers to time as seasonal counts.

Hence, while the results so far show that sulfur emissions are not yet making an impact on aerosol acidity or the neutralization ratio on a national level as was expected, interestingly, for both networks, the only areas with statistically significant pH trends, OAK and California, did not have statistically significant SO_4^{2-} trends, (though annual average SO_4^{2-} levels did decrease). However, with regards to Oak Grove, Mississippi, two things that stand out when compared to the other SEARCH sites is that first, the estimated yearly rate of NO_3^- increase of +92% per year (although statistically insignificant) was substantial, and secondly, that the rate increase of gaseous ammonia and its molar ratio were considerably higher than all the other SEARCH sites. In California, while there were no noticeable rates or ratios that stood out from the other regions, it had a fairly low amount of SO_4^{2-} at the start of the trend and was the region with the second lowest SO_4^{2-} throughout (Figure E.4c). For instance, while quite a few regions in the CASTNET/AMoN network had starting trend values well over 2 µg/m^3 for SO_4^{2-}, the reported starting trend values for the Rocky Mountains and California were 0.58 µg/m^3 and 1.1 µg/m^3. In addition, as shown in Figure E.4e, California had much higher levels of ammonia than any of the other regions. Therefore, the combination of low particulate SO_4^{2-} concentration and considerably higher gaseous ammonia levels might be the reason why responses to pH were seen more readily in California than in others. Similarly, Oak Grove, Mississippi also had the lowest SO_4^{2-} concentration out of all the SEARCH sites (except PNS), although not considerably lower than CTR. Thus, the common factor between OAK and California appears to be a combination of lower SO_4^{2-} levels, abundant ammonia, or higher rates of ammonia molar fraction and level increase.

The potential coupled effect of low SO_4^{2-} concentrations and high ammonia on pH is further illustrated by the results from the following SEARCH sites: JST, YRK, and BHM. All three sites had higher ammonia concentration levels and molar ratios of ammonia than OAK (Figures E.5e and E.5g), yet no significant improvements in pH were observed at those sites. In addition, starting SO_4^{2-} levels (based

on the intercept) at all three sites were substantially higher than at OAK. So it appears that even if ammonia emissions were to remain stable or increase as projected in some studies (Behera et al. 2013), it would not have a significant influence on aerosol acidity as long as SO_4^{2-} levels remain high.

Another possible explanation for why not much pH change was observed can be found in a study by Huang and colleagues (2011). In the study, they found that while significant changes and low free acidity (H^+ ions) were observed at molar ratios of NH_4^+/SO_4^{2-} greater than 1.5, the presence of acidity was not due to free SO_4^{2-} ions but bisulfate. Upon further investigation, they also noticed that the kinetic rates of SO_4^{2-} neutralization slowed significantly at ratios higher than 1.5, while the rate of ammonium NO_3^- formation shot up significantly, meaning that the presence of NO_3^- overtakes the neutralization of any SO_4^{2-} at ratios above 1.5. The study concludes that as long as NO_3^- is present, and in spite of high ammonia levels, aerosols will always have some acidity to them because neutralization is being taken over by NO_3^- and thus, the conversion of SO_4^{2-} from bisulfate will not take place due to the presence of NO_3^-. It is fair to note, however, that the studies conducted by Huang and colleagues (2011) took place in China where the concentration profile in the ambient air could have different effects on the results, and whether the presence of NO_3^- is higher in those cases is unclear. However, there is no evidence that excess production of ammonium nitrate took place here, as evidenced by the results from time-series trends, and the results show that the concentration of ammonium was affected by the presence of SO_4^{2-} and not NO_3^-. Furthermore, as pointed out by Weber and colleagues (2016), ammonium nitrate formation is largely unaffected at a pH below 3, and since the results from the linear intercept of the regression for mean seasonal pH show all sites with substantially low pH (except MW), no NO_3^- formation is likely to be taking place. Therefore, there is no reason to suppose that the exact same phenomenon is happening here.

The analysis of the results shows a relatively steady pH trend in spite of significant SO_4^{2-} reductions, and NO_3^- levels remain constant due to continued low pHs. However, it could be argued that the reason why the pH trends were, for the most part, statistically insignificant could be the short time-span of data used in this study. For unlike other studies such as those by Saylor and colleagues (2015) (9 yrs), and Weber and colleagues (2016) (15 yrs) where the data were collected over a much longer period, the data set in this study, for both CASTNET and SEARCH ranged only between four to seven years. However, the reason for the limited data, like in the case of CASTNET for instance, was that it had to be coupled with the AMoN data, which for the most part was not expanded to most regions until 2011, thereby limiting the number of data points available for study.

As we wanted to perform a comprehensive nationwide study of aerosol acidity with thermodynamic modeling, it meant starting from the year 2011 where more data points of AMoN could be coupled with CASTNET. A similar truncation of the data also had to be done with SEARCH, as the study required a full set of base cation and anions for use in the thermodynamic model, which was not available until

2008. However, despite the limited amount of data used from all three networks, similar trends in regards to ammonia and pH were also observed with the CMAQ results, which had a longer time trend (10 years). Therefore, this study corroborates and extends what was found by Weber and colleagues (2016) and further supports that aerosol pH has been impacted little by reductions in sulfur and nitrogen oxide emissions.

REFERENCES

Abbatt JPD, Benz S, Cziczo DJ, Kanji Z, Lohmann U, Mohler O. 2006. Solid ammonium sulfate aerosols as ice nuclei: A pathway for cirrus cloud formation. Science 313(5794):1770–1773.

Behera SN, Sharma M, Aneja VP, Balasubramanian R. 2013. Ammonia in the atmosphere: a review on emission sources, atmospheric chemistry and deposition on terrestrial bodies. Environmental Science and Pollution Research 20(11):8092–8131.

Blanchard CL, Hidy GM, Tanenbaum S, Edgerton ES, Hartsell BE. 2013. The Southeastern Aerosol Research and Characterization (SEARCH) study: Temporal trends in gas and PM concentrations and composition, 1999–2010. Journal of the Air & Waste Management Association 63(3): 247–259.

Blanchard CL, Tanenbaum S, Motallebi N. 2011. Spatial and temporal characterization of $PM_{2.5}$ mass concentrations in California, 1980–2007. Journal of the Air & Waste Management Association 61(3):339–351.

Byun D, Schere KL. 2006. Review of the governing equations, computational algorithms, and other components of the models-3 Community Multiscale Air Quality (CMAQ) modeling system. Applied Mechanics Reviews 59(2):51–77.

Charlson RJ, Schwartz SE, Hales JM, Cess RD, Coakley JA, Hansen JE, et al. 1992. Climate forcing by anthropogenic aerosols. Science 255(5043):423–430.

CMAS Center 2013. SMOKE version 3.5.1. The Institute for the Environment – The University of North Carolina at Chapel Hill. Available: *www.cmascenter.org/help/documentation.cfm?model=smoke&version=3.5.1*.

Delfino RJ, Sioutas C, Malik S. 2005. Potential role of ultrafine particles in associations between airborne particle mass and cardiovascular health. Environmental Health Perspectives 113(8):934–946.

Edgerton ES, Hartsell BE, Saylor RD, Jansen JJ, Hansen DA, Hidy GM. 2005. The Southeastern Aerosol Research and Characterization Study: Part II. Filter-based measurements of fine and coarse particulate matter mass and composition. J Air Waste Manag Assoc 55:1527–1542.

Fan SM, Jacob DJ. 1992. Surface ozone depletion in arctic spring sustained by bromine reactions on aerosols. Nature 359(6395):522–524.

Fisher JA, Jacob DJ, Wang QQ, Bahreini R, Carouge CC, Cubison MJ, et al. 2011. Sources, distribution, and acidity of sulfate-ammonium aerosol in the Arctic in winter-spring. Atmospheric Environment 45(39): 7301–7318.

Fountoukis C, Nenes A. 2007. ISORROPIA II: a computationally efficient thermodynamic equilibrium model for K^+–Ca^{2+}–Mg^{2+}–NH^{4+}–Na^+–SO_4^{2-}–NO_3^-–Cl^-–H_2O aerosols. Atmospheric Chemistry and Physics 7(17):4639–4659.

Ghio AJ, Carraway MS, Madden MC. 2012. Composition of air pollution particles and oxidative stress in cells, tissues, and living systems. Journal of Toxicology and Environmental Health, Part B 15(1):1–21.

Huang X, Qiu R, Chan CK, Kant PR. 2011. Evidence of high $PM_{2.5}$ strong acidity in ammonia-rich atmosphere of Guangzhou, China: Transition in pathways of ambient ammonia to form aerosol ammonium at NH_4^+/SO_4^{2-}=1.5. Atmospheric Research 99(3-4):488–495.

Kim YP, Seinfeld JH, Saxena P. 1993. Atmospheric gas aerosol equilibrium 1. Thermodynamic model. Aerosol Science and Technology 19(2):157–181.

Kleinman MT, Phalen RF, Mautz WJ, Mannix RC, Mcclure TR, Crocker TT. 1989. Health-effects of acid aerosols formed by atmospheric mixtures. Environmental Health Perspectives 79:137–145.

Lipfert FW, Wyzga RE. 1993. On the spatial and temporal variability of aerosol acidity and sulfate concentration. Journal of the Air & Waste Management Association 43(4):489–491.

Martin ST, Hung HM, Park RJ, Jacob DJ, Spurr RJD, Chance KV, et al. 2004. Effects of the physical state of tropospheric ammonium-sulfate-nitrate particles on global aerosol direct radiative forcing. Atmospheric Chemistry and Physics 4:183–214.

Meskhidze N, Chameides WL, Nenes A, Chen G. 2003. Iron mobilization in mineral dust: Can anthropogenic SO_2 emissions affect ocean productivity? Geophysical Research Letters 30(21):2085.

Nenes A, Pandis SN, Pilinis C. 1998. ISORROPIA: A new thermodynamic equilibrium model for multiphase multicomponent inorganic aerosols. Aquatic Geochemistry 4(1):123–152.

Pathak RK, Louie PKK, Chan CK. 2004. Characteristics of aerosol acidity in Hong Kong. Atmospheric Environment 38(19):2965–2974.

Pope CA, Dockery DW. 2006. Health effects of fine particulate air pollution: Lines that connect. Journal of the Air & Waste Management Association 56(6):709–742.

Ritter C, Notholt J, Fischer J, Rathke C. 2005. Direct thermal radiative forcing of tropospheric aerosol in the Arctic measured by ground based infrared spectrometry. Geophysical Research Letters 32(23).

Saylor R, Myles L, Sibble D, Caldwell J, Xing J. 2015. Recent trends in gas-phase ammonia and $PM_{2.5}$ ammonium in the Southeast United States. Journal of the Air & Waste Management Association 65(3):347–357.

Skamarock WC, Klemp JB, Dudhia J, Gill DO, Barker DM, Duda MG, et al. 2008. A Description of the Advanced Research WRF Version 3. NCAR Tech. Note NCAR/TN-475+STR. *http://opensky.ucar.edu/islandora/object/technotes:500*.

Thurston GD, Ito K, Hayes CG, Bates DV, Lippmann M. 1994. Respiratory hospital admissions and summertime haze air pollution in Toronto, Ontario: Consideration of the role of acid aerosols. Environmental Research 65(2): 271–290.

U.S. Environmental Protection Agency. 2014. 2011 Version 6 Air Emissions Modeling Platforms. Washington, DC:Office of Air and Radiation. Office of Air Quality Planning and Standards. Air Quality Assessment Division. Available: *www.epa.gov/air-emissions-modeling/2011-version-60-platform*.

U.S. Environmental Protection Agency. 2016. Clean Air Status and Trends Network (CASTNET) and the National Atmospheric Deposition Program (NADP). Available: *www.epa.gov/castnet/*.

Utell MJ. 1985. Effects of inhaled acid aerosols on lung-mechanics — an analysis of human exposure studies. Environmental Health Perspectives 63(Nov):39–44.

Utell MJ, Frampton MW. 2000. Acute health effects of ambient air pollution: The ultrafine particle hypothesis. Journal of Aerosol Medicine-Deposition Clearance and Effects in the Lung 13(4):355–359.

Valavanidis A., Fiotakis K, Vlachogianni T. 2008. Airborne particulate matter and human health: toxicological assessment and importance of size and composition of particles for oxidative damage and carcinogenic mechanisms. Journal of Environmental Science and Health Part C-Environmental Carcinogenesis & Ecotoxicology Reviews 26(4):339–362.

Weber RJ, Guo H, Russell AG, Nenes A. 2016. High aerosol acidity despite declining atmospheric sulfate concentrations over the past 15 years. Nature Geosci 9(4):282–285.

Wexler AS. 1991. Second-generation inorganic aerosol model. Atmospheric Environment 25A(12).

Xu L, Guo H, Boyd CM, Klein M, Bougiatioti A, Cerully KM, et al. 2015. Effects of anthropogenic emissions on aerosol formation from isoprene and monoterpenes in the southeastern United States. Proceedings of the National Academy of Sciences 112(1):37–42.

Zhang XL, Rao RZ, Huang YB, Mao M, Berg MJ, Sun WB. 2015. Black carbon aerosols in urban central China. Journal of Quantitative Spectroscopy & Radiative Transfer 150:3–11.

SUPPLEMENTAL TABLES

Table E.S1. Co-located CASTNET and AMoN sites by regions. CASTNET site measurements follow the start date of co-located AMoN site. Longitude and Latitude refer to the location of the CASTNET sites.

Amon	CASTNET	Region	State	CASTNET Site	Longitude	Latitude
CA67	JOT403	California	CA	Joshua Tree NP	34.069569	−116.38893
CA83	SEK430	California	CA	Sequoia NP - Ash Mountain	36.489469	−118.82915
CA44	YOS404	California	CA	Yosemite NP - Turtleback Dome	37.713251	−119.7062
IL46	ALH157	Midwest	IL	Alhambra	38.869001	−89.622815
IL11	BVL130	Midwest	IL	Bondville	40.051981	−88.372495
IL37	STK138	Midwest	IL	Stockton	42.287216	−89.99995
OH54	DCP114	Midwest	OH	Deer Creek	39.635888	−83.260563
KS31	KNZ184	Midwest	KS	Konza Prairie	39.10216	−96.609583
WI35	PRK134	Midwest	WI	Perkinstown	45.206525	−90.597209
NE98	SAN189	Midwest	NE	Santee Sioux	42.829154	−97.854128
CT15	ABT147	Northeast	CT	Abington	41.84046	−72.010368
PA00	ARE128	Northeast	PA	Arendtsville	39.923241	−77.307863
NY67	CTH110	Northeast	NY	Connecticut Hill	42.400875	−76.653516
PA29	KEF112	Northeast	PA	Kane Exp. Forest	41.598119	−78.767866
NJ98	WSP144	Northeast	NJ	Wash. Crossing	40.312303	−74.872663
MD99	BEL116	Northeast	MD	Beltsville	39.028177	−76.817127
CO88	ROM206	Rocky Mountains	CO	Rocky Mtn NP Collocated	40.278129	−105.54564
NC06	BFT142	Southeast	NC	Beaufort	34.884668	−76.620666
AR03	CAD150	Southeast	AR	Caddo Valley	34.179278	−93.098755
KY98	CDZ171	Southeast	KY	Cadiz	36.784053	−87.85015
NC26	CND125	Southeast	NC	Candor	35.26333	−79.83754
NC25	COW137	Southeast	NC	Coweeta	35.060527	−83.43034
FL11	EVE419	Southeast	FL	Everglades NP	25.391223	−80.680819
GA41	GAS153	Southeast	GA	Georgia Station	33.181173	−84.410054
FL19	IRL141	Southeast	FL	Indian River Lagoon	27.849215	−80.455595
KY03	MCK131	Southeast	KY	Mackville	37.704678	−85.048706
WV18	PAR107	Southeast	WV	Parsons	39.090434	−79.661742
VA24	PED108	Southeast	VA	Prince Edward	37.165222	−78.307067
AL99	SND152	Southeast	AL	Sand Mountain	34.289001	−85.970065
TN01	GRS420	Southeast	TN	Great Smoky NP - Look Rock	35.633482	−83.941606

Table E.S2. List of SEARCH sites, location, name and type (i.e., urban, rural, suburban)[a]

State/ Site Name	City Location	Type	Site Operating Timeline Start-End Date	Data collection Start /End Date	Seasons with insufficient data	No. of Seasons with data
GA/JST	Atlanta Jefferson St	Urban	8/01/98-NA	Spring '08/Winter '15	Spring '12, Summer '12, Fall '12	25
GA/YRK	Yorkville	Rural	5/6/98-NA	Spring '08/Winter '15	N/A	28
AL/BHM	N. Birmingham	Urban	10/23/98-NA	Spring '08/Winter '14	N/A	24
AL/CTR	Centreville	Rural	5/11/98-NA	Spring '08/Winter '14	Spring '11 Summer '11 Fall '11	21
MS/GFP	Gulfport	Urban	4/13/99-NA	Summer '08/Winter '11	Fall '08	10
MS/OAK	Oak Grove	Rural	5/16/98-12/13/10	Summer '08/Winter '11	N/A	11
FL/PNS	Pensacola	Urban	2/01/99-12/13/09	Summer '08/Winter '10	Spring '08	6
FL/OLF	Outlying Landing Field #8	Suburb	1/4/99-NA	Spring '08/Winter '15	Spring '11 Summer '11 Fall '11 All 2012 Winter '13	20

[a] The "Data Collection Start/End Date" reflects the seasons during which SEARCH data for base cations (Mg^{2+}, Na^{+}, Ca^{2+} and K^{+}) are available. Certain ion data are unavailable during seasons shown in "Seasons with insufficient data".

ABBREVIATIONS AND OTHER TERMS

AMoN	Ammonia Monitoring Network
CA	California region
CASTNET	Clean Air Status and Trends network
CMAQ	Community Multiscale Air Quality
ISORROPIA II	a thermodynamic equilibrium model
MW	midwest region
NE	northeast region
NO_3^-	nitrate
NO_x	oxides of nitrogen
PM	particulate matter
$PM_{2.5}$	particulate matter ≤2.5 µm in aerodynamic diameter
RH	relative humidity

RK	Rocky Mountain region
SEARCH	SouthEastern Aerosol Research and Characterization
SO_4^{2-}	sulfate
SO_x	oxides of sulfur
SE	Southeast Region

SEARCH Sites

BHM	N. Birmingham, Alabama
CTR	Centreville, Alabama
GFP	Gulfport, Mississippi
JST	Jefferson Street, Atlanta, Georgia
OAK	Oak Grove, Mississippi
OLF	Outlying Landing Field #8, Florida
PNS	Pensacola, Florida
YRK	Yorkville, Georgia